


 Cite this: *RSC Adv.*, 2024, **14**, 35754

# LCST/UCST behavior of polysaccharides for hydrogel fabrication

 Seo Hyung Moon, †<sup>a</sup> Sol Ji Park, †<sup>a</sup> Ye Won Lee †<sup>a</sup> and Yun Jung Yang \*<sup>ab</sup>

Hydrogel-based scaffolds play a crucial role in widespread biotechnological applications by providing physicochemical stability to loaded cells or therapeutic agents, interacting with organismal microenvironments, and controlling cargo release. Polysaccharides are regarded as attractive candidates among substrate materials because of their high water-retaining capacity, reactive functional groups, ease of gelation, low immunogenicity, biodegradability, and biocompatibility. However, employing polysaccharide-based hydrogel scaffolds for practical use in response to ongoing physiological and pathological changes within the human body, such as insufficient mechanical strength, uncertain degradation, and uncontrollable release patterns, is challenging. Several physically noncovalent or chemically covalent crosslinking strategies have been utilized to modify the physicochemical properties and biofunctionality of polysaccharide-based hydrogels. Among them, thermo-responsive gelation systems have been considered a promising approach for fabricating advanced scaffolds, referred to as 'stimuli-responsive' or 'smart' hydrogels. This is because of the sol–gel transition with a single trigger, requiring no further environmental or chemical intervention, and *in situ* and reversible gelation under ambient physiological temperature changes in a minimally invasive manner. This review highlights the classification, reaction mechanisms, characteristics, and advanced studies on thermo-responsive polysaccharides exploited in various biomedical fields.

 Received 29th August 2024  
 Accepted 24th October 2024

DOI: 10.1039/d4ra06240j

[rsc.li/rsc-advances](https://rsc.li/rsc-advances)

## 1. Introduction

Biomedical engineering is a multidisciplinary field devoted to developing biological substitutes that replace, restore, and regenerate defective tissues by incorporating cells in fundamental construct matrices, known as scaffolds.<sup>1</sup> The scaffolds, porous three-dimensional matrices made of polymeric biomaterials, perform a crucial role as indispensable components of engineered tissues.<sup>2</sup> Scaffolds facilitate the incubation of cells and support their attachment, growth, proliferation, differentiation, and migration for the subsequent development of new tissue; provide chemical and physical stability in a physiological environment; and transport biochemical signals, nutrients, and oxygen.<sup>3</sup> To design suitable scaffolds for various biomedical applications, optimal parameters, such as adequate porosity (pore size and shape), controllable biodegradability without producing toxic byproducts, biocompatibility, rheological and mechanical properties, and surface characteristics (topography and roughness), must be tailored depending on the targeted tissue.<sup>3</sup> Hydrogel-based scaffolds, colloidal solids with hydrophilic polymer networks, are commonly used as soft tissue alternatives

because of their ECM-like architectures. They can be produced using synthetic polymers, natural polymers, and a blend of both.<sup>4</sup> The formation of a hydrogel involves physical, chemical, or hybrid bonding, which can be achieved through various methods such as radiation techniques, bulk polymerization, free radical polymerization, and solution casting.<sup>4</sup> Viscoelasticity, minimally invasive delivery of macromolecules to the damaged site, ability to swell readily without dissolving, and a high content of biological fluids (up to several thousand%) are its merits.<sup>2,5</sup>

Polysaccharides such as alginate, carrageenan, cellulose, chitosan, and hyaluronic acid have been regarded as (a) attractive candidate materials for transporting therapeutic cells; (b) small molecules; and (c) bioactive substances; thus facilitating pharmacological effects, including tissue repair and antitumor, antibacterial, and immune regulation effects, owing to their high water-retaining capacity, renewability, low immunogenicity, biodegradability, and biocompatibility.<sup>6,7</sup> In addition to their unique biological activities, many different polysaccharides and their derivatives with multiple structures and molecular weights above 100 kDa or even 1000 kDa allowed them to have a wide range of mechanical and rheological behaviors and potential gelatinization performances.<sup>8,9</sup> Compared with protein-based hydrogels, polysaccharide-based hydrogels can avoid rapid degradation by proteases *in vivo* and maintain structural integrity without shrinking, facilitating long-term tissue regeneration and sustained release of biomolecules.<sup>10,11</sup>

<sup>a</sup>Department of Biological Sciences and Bioengineering, Inha University, Incheon 22212, Republic of Korea. E-mail: yj.yang@inha.ac.kr

<sup>b</sup>Inha University Hospital, Incheon, 22332, Republic of Korea

† These authors contributed equally to this work.



However, employing polysaccharide-based hydrogel scaffolds for practical use in response to ongoing physiological and pathological changes within the human body is challenging; for example, insufficient mechanical strength, uncontrollable absorbency (correlated with loading capacity), and uncertain degradation (correlated with release patterns). To modify the physicochemical properties and biofunctionality of polysaccharide-based hydrogels, physically non-covalent or chemically covalent crosslinking strategies have been utilized.<sup>12</sup> Generally, noncovalent interactions such as host-guest metal coordination, nanofillers incorporation, hydrophilic/hydrophobic interactions, and hydrogen bonding have been applied to fabricate physical networks.<sup>13,14</sup> In contrast, a covalent network can be achieved by redox, photo-, thermal- or free radical polymerization.<sup>12</sup> Using these crosslinking strategies by engineering the intrinsic functional moieties of polysaccharides facilitated the design of advanced scaffold systems, referred to as 'intelligent' or 'smart' hydrogels.<sup>15</sup> Because they are responsive to external stimuli such as pH, incident light wavelength, temperature, enzymatic environment, ionic strength, and magnetic and electric fields, their biological and mechanical aspects can be enhanced depending on the desired applications.<sup>16</sup>

Thermo-responsive hydrogels that gelate *via* hydrophobic interactions have been widely exploited in biomedicine. This strategy allows a sol-gel transition with a single trigger, requiring no further environmental or chemical intervention.<sup>17</sup> This phase transition process demonstrates the separation of the solution and solid states at certain temperatures.<sup>18</sup> Thermogels can be divided into two types according to their phase separation behavior: critical solution temperature (CST), upper critical solution temperature (UCST), and lower critical solution temperature (LCST). The polymer remained soluble below the LCST. However, above the LCST, they become more hydrophobic and insoluble, leading to their solidification. In contrast, hydrogels that were solidified by cooling the polymer solution had a UCST.<sup>19</sup> These *in situ*- and reversible gel-forming systems can react to readily accessible physical and thermal stimuli, facilitating the delivery of biomaterials within a solution in a minimally invasive manner.<sup>20,21</sup> Owing to their phase transition ability, especially at

physiological temperatures, both thermo-responsive polysaccharide-based hydrogels have become promising platforms for biomedical applications such as regenerative medicine, targeted drug delivery, and implantation of artificial organs.<sup>16</sup>

This review discusses the intrinsic characteristics, fabrication methods, and reaction mechanisms of thermo-responsive hydrogels. The most extensively exploited thermo-responsive polysaccharides in tissue engineering applications have been classified into two groups: UCST-types, including agarose and carrageenan, and gellan gum; LCST-types, including chitosan, xyloglucan, and methylcellulose. Additionally, recent studies on strategies to promote tissue specificity for targeted performance in various biomedical applications, including *in situ* gel-based drug delivery (ocular, nasal, osteogenic, and topical lesion site), photo-thermal therapy, tissue regeneration (cartilage, bone, and skin wound dressing), and 3D cellular scaffold engineering of each material, are discussed to enhance the readers' understanding.

## 2. UCST-responsive polysaccharides

UCST hydrogels primarily consist of hydrophilic components, and their swelling ability increases in aqueous solutions with temperature increases<sup>18</sup> (Fig. 1(A)). Entropy-driven dehydration and collapse of the polymer matrix lead to a gel state at temperatures below the UCST.<sup>22</sup> Their phase transition temperatures vary between polymers; however, most transition to a liquid state at 60–70 °C, and gelation occurs at physiological temperatures of 25–35 °C.

Carrageenans, agarose, and gellan gums belong to UCST-type polysaccharides,<sup>23</sup> which have been extensively studied in biomedical applications due to their similarity to the glycosaminoglycan composition of the ECM, low immunogenicity, innate biocompatibility, and encapsulating capability of living cells by gaining shear thinning behavior.<sup>24,25</sup> Both carrageenans and gellan gums undergo a transition from a disordered state (random coil) to an ordered state (helix) to form a physical gel, followed by the aggregation of helical segments into extended network junctions.<sup>26</sup> Carrageenan has a wide range of critical

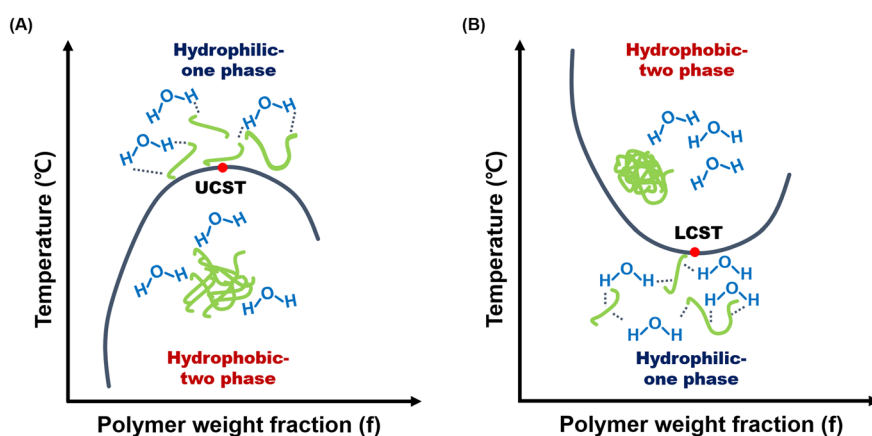


Fig. 1 Phase diagrams of (A) UCST and (B) LCST properties of thermo-responsive polysaccharides.<sup>23,86,87</sup>



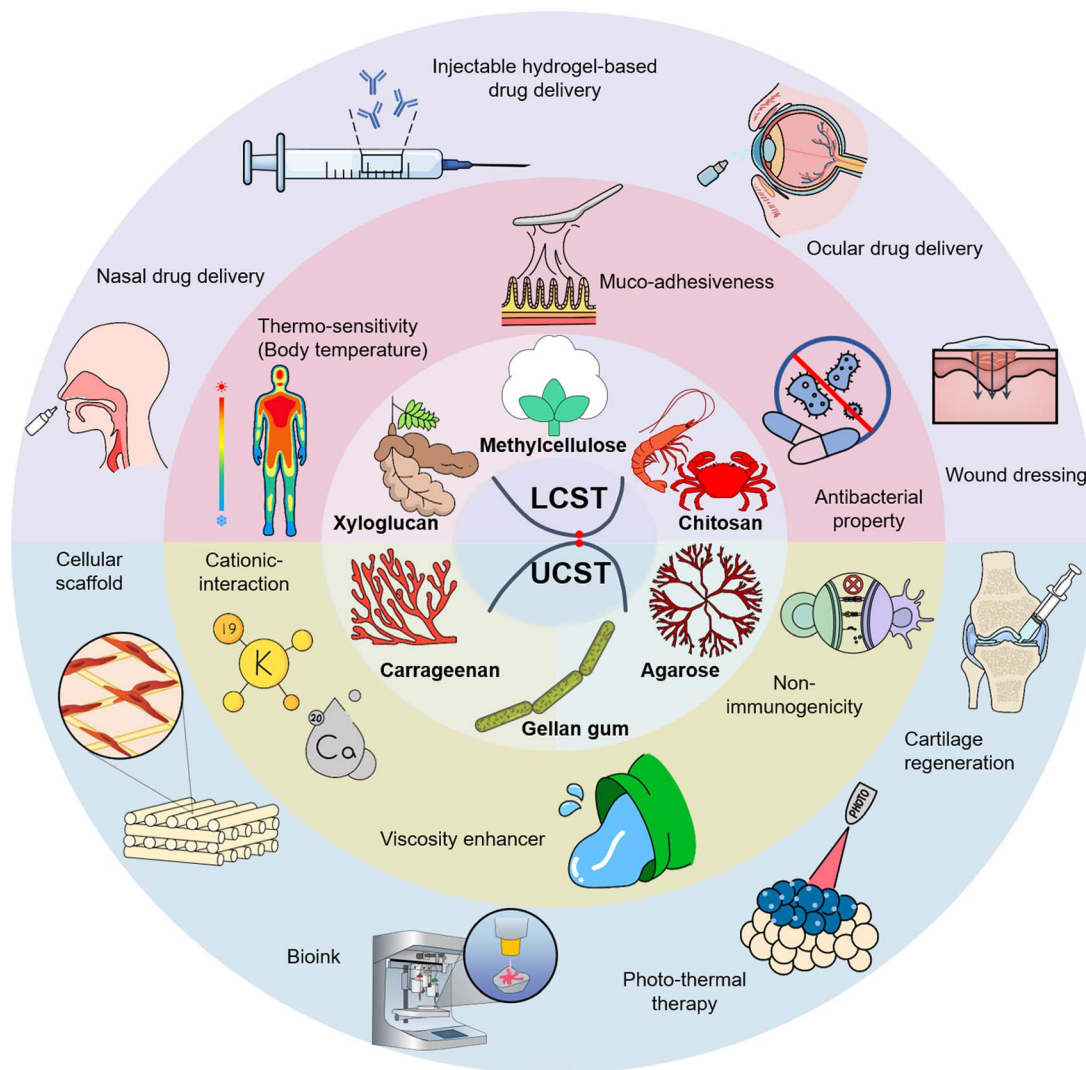


Fig. 2 A comprehensive review of thermo-responsive polysaccharides in biomedical applications.

transition temperatures, from 35 to 65 °C,<sup>27,28</sup> while the gellan gum typically transitions around 30 to 40 °C.<sup>29</sup> Especially for carrageenan, anionic sulfate groups in carrageenan make it highly sensitive to cationic surroundings (mono- or di-valent cations), promoting the formation of helical aggregates.<sup>30</sup> Unlike anionic carrageenans, agarose is a neutral polysaccharide, facilitating gelation without counterions or other additives.<sup>31</sup> As the agarose solution, which remains in sol state at above 60 °C, begins to cool, intramolecular hydrogen bonds form, creating a single helix structure that makes the agarose chains more rigid.<sup>31</sup> With further cooling, intermolecular bonds between the single helices lead to the formation of double helices, producing a gel network in double helical aggregates. The sol–gel transition kinetics in these UCST-responsive polysaccharide gels and their gelation conditions affect the microstructure, pore size, rheological properties, and thermal stability of the gels.<sup>31</sup>

Thermo-responsive hydrogels with UCST present a promising avenue for biomedical applications owing to their facile

control over physical properties *via* gelation mechanisms.<sup>32</sup> In particular, their ability to modulate their properties during preparation renders them highly suitable for biomedical applications, offering versatility across various tissues and organs (Fig. 2). Moreover, their characteristic transition from the solution to the gel phase above a critical temperature makes them ideal candidates for therapeutic strategies such as photothermal therapy. UCST-based photothermal therapy hydrogels can release on-demand therapeutic agents at specific target sites.<sup>33</sup> Additionally, the ease of formulation of UCST hydrogels allows the adjustment of gelation temperature ranges, making them suitable for diverse applications, including 3D bioprinting, scaffolds for tissue regeneration, wound dressing, and drug delivery vehicles for photo-thermal therapy. This review highlights the significant potential of UCST hydrogels as versatile biomaterials for advancing biomedical research, focusing on agarose, carrageenan, and gellan gums, both exhibiting UCST behavior (Table 1).





**Table 1** Summary of UCST-responsive polysaccharides used in biomedical applications

Polysaccharides	Structures	Characteristics	UCST range (°C)	Biomedical applications	References
Agarose		<ul style="list-style-type: none"> <li>• <i>In situ</i> gelation</li> <li>• Promoting cartilage regeneration</li> <li>• Photo-thermal responsiveness</li> <li>• Non-immunogenicity</li> </ul>	30–40	<ul style="list-style-type: none"> <li>• Scaffold for cartilage regeneration</li> <li>• Photo-thermal drug carrier</li> </ul>	34, 36, 41–43 and 45
Carrageenan	 Kappa-  Iota-  Lamda-	<ul style="list-style-type: none"> <li>• Gelation ability</li> </ul> <p>(cation, weight fraction)</p> <ul style="list-style-type: none"> <li>• Shear-thinning behavior</li> </ul>	35–65	<ul style="list-style-type: none"> <li>• 3D cellular scaffold</li> </ul>	27, 53, 55, 58, 61–63 and 69
Gellan gum		<ul style="list-style-type: none"> <li>• Modulate mechanical property</li> <li>• Gelation ability (mono, di, trivalent ions)</li> <li>• Tunable gelation temperature</li> <li>• Photo-thermal responsiveness</li> </ul>	37.5	<ul style="list-style-type: none"> <li>• Injectable hydrogel for wound healing</li> <li>• Temperature-sensitive therapeutics carrier</li> <li>• Photo-thermal drug carrier</li> </ul>	76, 77, 80, 83, 85, 88 and 89

## 2.1. Agarose

Agarose is a thermo-responsive polysaccharide dissolved at a high temperature of 70–100 °C to have a sol and a gel state in a low-temperature range of 30–40 °C to exhibit UCST behavior.<sup>34</sup> It can be purified from agar sources such as red algae, which can be easily produced in many countries cost-effectively.<sup>35,36</sup> Owing to its non-immunogenic properties and thermo-responsive reactivity, agarose is actively used in tissue engineering.<sup>37</sup> Agarose has  $\beta$ -D-galactose and 3,6-anhydro- $\alpha$ -L-galactose in its structure, linked by  $\alpha$ -(1 → 3) and  $\beta$ -(1 → 4) glycosidic bonds.<sup>38</sup> Due to numerous hydroxyl groups in  $\beta$ -D-galactose, agarose readily interacts with hydrogen atoms, forming hydrogen bonds.<sup>39</sup> This interaction allows the structure to transition from a random coil to a helical structure in response to temperature changes, resulting in a physical three-dimensional network.<sup>40</sup>

The thermo-responsive properties of agarose make it suitable for application as an injectable hydrogel-based scaffold material. Agarose can encapsulate some biomolecules in a sol state at elevated temperatures and rapidly transition to a gel state at the physiological temperature of 37 °C. In the case of irregular defects in the cartilage area, agarose can effectively promote the treatment of damaged cartilage areas as support with stable mechanical properties while tightly filling the defect area according to temperature reactivity characteristics.<sup>41</sup> An agarose injectable hydrogel encapsulated autologous bone marrow mesenchymal stem cells (BMSCs) to repair micro defects in the articular cartilage.<sup>42</sup> This agarose-based injectable hydrogel filled the irregular and micro-defect areas, promoted the adhesion and proliferation of chondroitin cells, and facilitated the integration between the newly formed and existing cartilage tissues, achieving a good distribution of chondrocytes in the defect area.

Additionally, the UCST behavior of agarose can be utilized as a drug delivery carrier in photo-thermal cancer therapy. Agarose exhibits a gel phase at the physiological temperature of 37 °C and a sol state in response to increased temperatures. This property is suitable for implementing on-demand drug release behavior in response to increased temperatures induced by photo-irradiation.<sup>43,44</sup> Agarose has been used as a carrier for photo-thermal drug delivery by blending it with hydrophilic polymers such as cellulose to enhance its mechanical

strength.<sup>45</sup> When combined with hydrophilic polymers containing abundant hydroxyl groups, agarose forms physical crosslinks with polymers with enhanced compressive strength and elastic modulus. This enhanced mechanical strength allowed the blended agarose hydrogel to specifically release drugs only when irradiated with light, making it advantageous for applications in targeted drug delivery. This thermo-responsive agarose hydrogel undergoes a sol-gel transition when the temperature changes, allowing it to rapidly respond to an increase in temperature caused by photo-irradiation, dissociating physical crosslinking with the release of drugs, and achieving over 80% cancer cell mortality.

Agarose, which exhibits thermo-responsive phase-transition properties, can also be utilized as a delivery vehicle for cancer therapy. Agarose-based injectable hydrogels demonstrate effective drug delivery capabilities for tumor sites requiring localized treatment by modulating release kinetics with a low melting point. In particular, the photo-thermal sol-gel transition behavior of agarose, characterized by its UCST, enables on-demand drug release, making it highly suitable for applications in cancer treatments that necessitate controlled drug release. Agarose hydrogel was employed as a photo-thermal drug carrier to deliver doxorubicin to tumor sites.<sup>43</sup> Upon near-infrared irradiation, the on-demand release profile was observed (Fig. 3(A)). When the treatment effect was confirmed for the tumor model mouse *in vivo*, the tumor suppression rate reached 97.5%. For solid tumors, the agarose hydrogel-treated group exhibited approximately 9 times higher tumor death rate compared to the untreated group (Fig. 3(B)). These results suggest that agarose-based UCST hydrogels hold significant potential as a localized chemo-photo-thermal therapeutic platform for tumor treatment.

## 2.2. Carrageenan

Carrageenan is a thermo-responsive polysaccharide exhibiting a UCST behavior that is converted to sol in a high-temperature state and gel in a low-temperature state within the temperature range of 35–65 °C.<sup>27,28</sup> The sulfate ester content on each carrageenan backbone ranges from 15% to 40%, classifying it into three types: kappa ( $\kappa$ ), iota ( $\iota$ ), and lambda ( $\lambda$ ), based on the number and position of the sulfate groups.<sup>46–50</sup> The kappa-, iota-

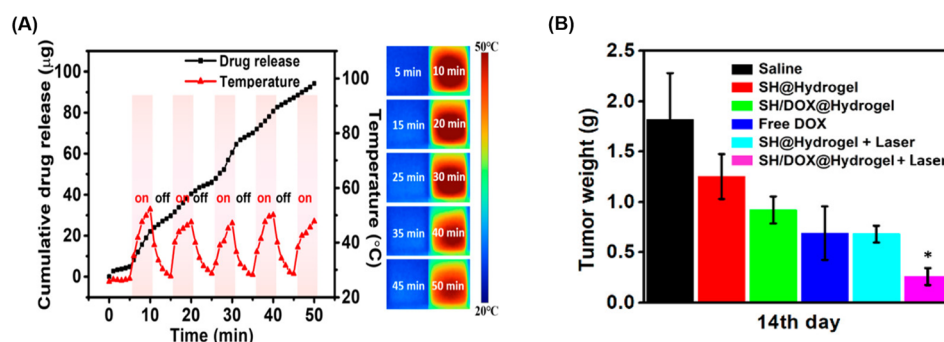


Fig. 3 (A) Controllable doxorubicin release induced by photo-thermal effects irradiated by near-infrared and (B) the comparison of the average weight of excised tumors after various treatments. Reprinted with permission from ref. 43. Copyright (2018) American Chemical Society.



, and lambda-carrageenans possess one, two, and three sulfate groups, respectively.<sup>51</sup> An increase in the number of ester sulfate groups correlates with a reduced gel strength and decreased solubility temperature.<sup>52</sup> The gelation properties of carrageenan are cation-dependent, with cations such as  $K^+$  and  $Ca^{2+}$  influencing both gel formation and the gel-sol transition temperature based on their concentration.<sup>53</sup> In the gel formation process of carrageenans, the interaction between the sulfate group and the cation diminishes the electrostatic repulsion among the polysaccharide chains, resulting in the adoption of a double helical structure by the chain.<sup>54,55</sup>

Based on these characteristics, carrageenan can modulate mechanical strength and rigidity through the number of sulfate groups and cation concentration, enabling the production of printable hydrogels with excellent crosslinking ability, tunable cell orientation, and fluid properties, making it highly suitable for tissue engineering applications.<sup>50,56</sup> Methacrylated kappa carrageenan and alginate were combined to create a bio-printable, dual-crosslinked hydrogel.<sup>55</sup> The sulfate group of carrageenan promoted cell adhesion, proliferation, and differentiation, whereas its gelation properties allowed for the extrusion of high-concentration bioink under low pressure, minimizing the impact of shear force on cell viability.<sup>57,58</sup> In addition, gelling molecules clustered better with alginate and kappa-carrageenan, reducing electrostatic interactions.<sup>59</sup> Calcium ions added for double crosslinking enhanced the helical structure aggregation of carrageenan by alleviating sulfate group repulsion.<sup>60</sup> The gel properties became possible at physiological temperatures, maximizing cell orientation, proliferation, and adhesion on the sample surface, providing a conducive environment for stable cell growth.<sup>55</sup>

By employing the thermo-responsive properties of carrageenan, the scaffold effectively addressed the limitations of existing protein scaffolds.<sup>61</sup> A cell-friendly ink was generated by incorporating Iota-carrageenan with silk fibroin, enhancing the ink viscosity compared to pure protein formulations and facilitating 3D printing processes. Carrageenan-based ink, characterized by its shear-thinning<sup>62,63</sup> behavior, enhances cell viability during extrusion, a notable improvement over traditional fluid inks (Fig. 4). Scaffolds mixed with carrageenan exhibit minimal shrinkage<sup>64</sup> over prolonged culture periods, presenting an advantage over scaffolds composed solely of proteins. Typically, proteins depend on covalent bonds for binding, whereas carrageenan mixing introduces physical crosslinking, which leads to double crosslinking.<sup>61</sup> Additionally, the temperature-responsive gelation of carrageenan imparts non-Newtonian fluid properties to the ink, ensuring uniform cell encapsulation and distribution throughout the printing process and enhancing the overall scaffold functionality and performance.<sup>65-68</sup>

Besides being used as ink, injectable hydrogels find application in wound healing and tissue repair. A kappa and iota carrageenan blend with locust bean gum and gelatin yielded an injectable hydrogel.<sup>69</sup> Gelatin's numerous amino groups foster electrostatic interactions with carrageenan, forming a polymer electrolyte composite, stabilizing the carrageenan network, enhancing mechanical strength, and increasing carrageenan content.<sup>70,71</sup> Unlike individual iota and kappa carrageenan gels, the mixed gel displayed modified co-aggregation and formed a mutually penetrating network, surpassing the combined rigidity of each gel component. This underscores the advantage of using mixed carrageenan over individual types.<sup>72</sup> Due to its

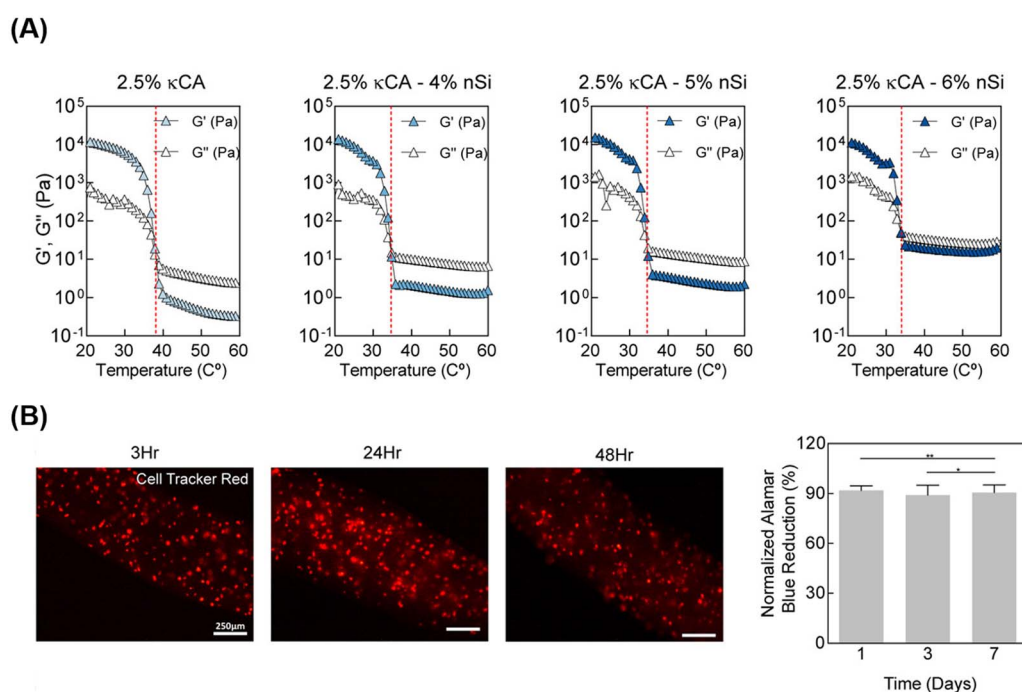


Fig. 4 (A) Rheological analysis of carrageenan-based bioinks in temperature sweep mode and (B) fluorescent images demonstrating cells evenly distributed in fibers. Reprinted with permission from ref. 63. Copyright (2017) American Chemical Society.





highlight the potential of gellan gum hydrogels to preserve the bioactivity of temperature-sensitive molecules such as antibodies while enabling prolonged drug delivery.

Gellan gum with UCST responsiveness can be used as a hydrogel biomaterial for photo-thermal therapy. Effective treatment of bacterial infectious chronic wounds requires antibacterial activity and the design of a treatment vehicle capable of preventing further infections.<sup>84</sup> Photo-thermal therapy is a promising approach for treating infectious wounds, as the localized temperature increase induced by light irradiation can directly facilitate the destruction of fungal pathogens. Gellan gum, which undergoes a phase transition in response to temperature changes, can be applied as a wound dressing material for photo-thermal-assisted infectious wound healing.<sup>85</sup> Upon the infectious wounds, the photo-/thermo-reactive on-off drug release capability and antibacterial treatment ability of the gellan gum hydrogel were confirmed. It exhibited on-off behavior in response to photo-thermal stimulation within a temperature range of 0–50 °C, with drug release capacity approximately 20% higher after 120 hours compared to the non-stimulated control group. Additionally, for the growth kinetics of two bacterial groups, the colony-forming units were significantly reduced relative to the control group without hydrogel. These results suggest the potential of a photo-thermal stimulation-responsive gellan gum hydrogel as a wound healing agent capable of preventing reinfection at chronic wound sites while promoting effective healing.

### 3. LCST-responsive polysaccharides

LCST hydrogels contain hydrophilic and hydrophobic groups and undergo sol–gel transitions depending on temperature changes.<sup>91</sup> When the temperature becomes below the LCST, the gels transform into highly viscous liquid or solution.<sup>92</sup> In contrast, polymers near the LCST undergo a reversible phase transition from soluble (random curl) to insoluble (crash or micelle form)<sup>93</sup> (Fig. 1(B)). This phase transition occurs at a physiological temperature of approximately 32–37 °C.

Typical polysaccharides exhibiting LCST behavior include chitosan, xyloglucan, and methylcellulose,<sup>23</sup> which have attracted significant attention in various biomedical applications due to their thermo-sensitivity under physiological temperatures, non-toxicity, injectability as biological transporters to lesion sites, bioadhesives, and antimicrobial properties.<sup>23,24</sup> When heated from 5 to 70 °C, chitosan-based aqueous solutions in the presence of disodium  $\beta$ -glycerophosphate ( $\beta$ -GP) simultaneously turn into a gel at 37 °C.<sup>94,95</sup> Upon cooling, the reverse process occurs (gel to solution), demonstrating the thermo-reversibility of the gel.<sup>96</sup> Xyloglucan, with 35–50% of its galactose residues removed by using  $\beta$ -galactosidase, has an optimized sol–gel transition temperature that depends on the concentration of pre-gel solution.<sup>97,98</sup> A higher galactose removal ratio broadens the gelation temperature range to 22–35 °C.<sup>98,99</sup> The critical transition temperature of methylcellulose, ranging between 60 and 80 °C, hinders its thermal transition at physiological temperature.<sup>100</sup> However, several factors, such as substitution degree of methylation, concentration, and addition

of anions, sugars, and sugar alcohols, can adjust its thermal gelation temperature to around 37 °C.<sup>23,101</sup> The macromolecular arrangement of these LCST-responsive polysaccharides changes from the hydrophilic (sol) to hydrophobic (gel) state when the temperature exceeds their respective LCST.<sup>102</sup> In particular, for methylcellulose, hydroxyl groups (–OH) and water molecules interact through hydrogen bonds below the LCST, resulting in the hydration of methylcellulose chains in solution. These hydration layers form around methyl groups (–OCH<sub>3</sub>), preventing hydrophobic interactions.<sup>103</sup> When the methylcellulose solution absorbs thermal energy as the temperature rises above LCST, the hydration layers diminish, and inter-/intra-molecular hydrophobic interactions form simultaneously, forming a physically crosslinked gel.<sup>104</sup>

Hydrogels exhibiting LCST offer a unique advantage in biomedical applications because of their ability to induce *in situ* gelation at physiological temperatures, facilitating the minimally invasive delivery of hydrogel matrices into the body. This property makes them particularly suitable injectable hydrogels, presenting distinctive and crucial points.<sup>105</sup> Furthermore, the capacity for gelation at a physiological temperature of 37 °C makes LCST-based hydrogels suitable for cell-culture applications. LCST-based cell sheets can serve as stable scaffolds for cell culture at 37 °C, allowing for the robust manipulation of cell layers by simply changing the temperature.<sup>106</sup> Consequently, LCST-based hydrogels have potential applications as 3D cell sheets, tissue regeneration scaffolds, and *in situ* gel-based drug delivery systems for ocular, dermal, osteogenic, nasal, and topical lesion sites. This study examined the advantages and applications of LCST hydrogels in biomedical research and therapeutic interventions, focusing on the typical polysaccharides that exhibit LCST behavior: chitosan, xyloglucan, and methylcellulose (Table 2).

#### 3.1. Chitosan

Chitosan is another natural thermo-responsive polysaccharide. Chitosan exists in the sol state at 25 °C, and when the temperature is increased to 37 °C, it exhibits a gel phase owing to its LCST behavior. Chitosan has 2-amino-2-deoxy- $\beta$ -D-glucan in its structure, which is connected by glycosidic linkages.<sup>107</sup> Chitosan is derived from the hard shells of crustaceans or insects.<sup>108</sup> Chitosan can be obtained through the deacetylation of the acetamide groups of chitin into primary amino groups, and the gelation ability is controlled by the degree of protonation of the amino groups induced through deacetylation.<sup>109</sup> The amine groups of chitosan can be adjusted to gelate under biological conditions, such as physiological temperature and neutral pH, by appropriately adding additives like  $\beta$ -GP, which is a type of salt that facilitates the electrostatic interactions with the amine groups of chitosan<sup>110</sup> (Fig. 6). Furthermore, chitosan has a positive charge, imparting polycationic properties. Consequently, chitosan can interact with various polyanionic materials.

Due to its structural properties and temperature responsiveness, chitosan can be utilized as a drug delivery vehicle. Chitosans' polycationic nature allows adhesion to anionic







Table 2 Summary of LCST-responsive polysaccharides used in biomedical applications

Polysaccharides	Structures	Characteristics	LCST range (°C)	Biomedical applications	References
Chitosan		<ul style="list-style-type: none"> <li>• Salt- induced phase transition</li> <li>• Antibacterial property</li> <li>• Muco-adhesiveness</li> </ul>	37	<ul style="list-style-type: none"> <li>• <i>In situ</i> gel-based drug delivery (ocular, wound dressing)</li> </ul>	110–112 and 114–116
Xyloglucan		<ul style="list-style-type: none"> <li>• Degalactosylation-induced phase transition</li> <li>• Promoting stem cell survival</li> <li>• Pseudo-plastic flow behavior</li> <li>• Thermo-sensitivity</li> </ul>	37	<ul style="list-style-type: none"> <li>• <i>In situ</i> gel-based drug delivery (nasal, stem cell)</li> <li>• <i>In situ</i> gel-based cellular scaffolds (osteogenic cell)</li> </ul>	97–99, 121–125, 127, 135, 136 and 138
Methylcellulose		<ul style="list-style-type: none"> <li>• Hydrophobic interaction-based gelation</li> <li>• Flexible shape and geometry</li> </ul>		<ul style="list-style-type: none"> <li>• Topical drug delivery</li> <li>• Bone tissue regeneration</li> <li>• 3D cellular scaffolds</li> </ul>	102, 144, 147, 153, 156 and 163

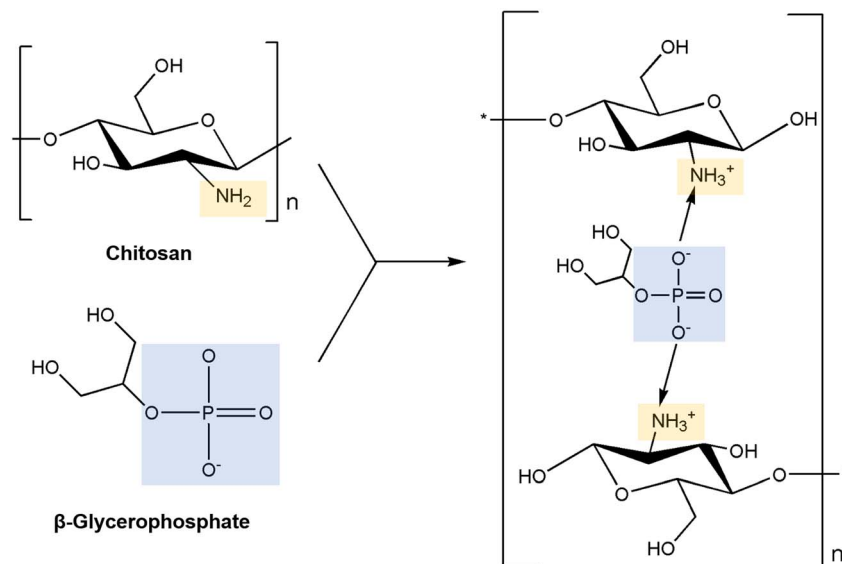


Fig. 6 The mechanism of neutralization of chitosan with  $\beta$ -glycerophosphate.<sup>110</sup>

mucosal surfaces.<sup>111,112</sup> Therefore, in the field of ocular drug delivery, thermo-responsive chitosan is capable of rapid gelation on the ocular surface, preventing the solution-phase formulation of ocular drugs from draining off the cornea and improving the drug uptake ratio.<sup>113</sup> Chitosan-based *in situ* hydrogels have been used as ocular drug delivery vehicles for treating bacterial conjunctivitis.<sup>114</sup> The chitosan hydrogel with an additive of  $\beta$ -GP rapidly undergoes gelation in 2 min, demonstrating the sustained release of ocular drug molecules by controlling the drug release amount from 95% to 83.3%. Additionally, it prolonged the residence time of the drug molecules on the ocular surface, providing a 38.4% higher drug efficacy than the solution-phase formulation of drug vehicles.

In addition, chitosan can be used as an injectable hydrogel-based wound-dressing material. The cationic chitosan interacts with negatively charged bacterial cell membranes, causing leakage of intracellular components and altering cell permeability.<sup>115</sup> This mechanism confers antibacterial and antifungal activities to chitosan. The temperature-responsive gelation properties of chitosan make it suitable as an injectable wound dressing. It can be injected in its sol state at 25 °C to fill irregularly shaped wounds and then gelled *in situ* at 37 °C. Chitosan-based injectable hydrogels are used as wound-dressing materials for treating chronic wounds caused by antibiotic-resistant bacteria.<sup>116</sup> When introduced in the sol state, chitosan closely covered the irregular wounds, significantly improving the suture rate of the infected wound area from 33% to 75%. Additionally, due to chitosan's antimicrobial characteristics, it suppressed the growth of antibiotic-resistant bacteria from 67.70% to 38.29%.

Chitosan, which exhibits LCST properties, can be utilized as a dressing material for chronic wounds requiring antibacterial activity. The high density of amine groups in the chitosan backbone enables double crosslinking through additional molecular modifications, enhancing its mechanical properties

and making it an effective carrier for therapeutic delivery. Chitosan, double-crosslinked with genipin, was developed to deliver therapeutic agents in wound healing applications.<sup>117</sup> This double-crosslinked, amine-modified chitosan demonstrated double 1.94 times enhanced compressive strength and stable injectability in the syringe. Thermo-responsive chitosan hydrogel gelled at 37 °C and provided sustained release of therapeutic agents, achieving low bacterial survival rates of  $32.9 \pm 6.0\%$  and  $24.2 \pm 2.6\%$  against *E. coli* and *S. aureus*, respectively, thereby demonstrating effective antibacterial activity. These results suggest that chitosan hydrogels possess robust thermo-gelling ability and substance release properties with stable delivery ability, making chitosan hydrogel an effective therapeutic delivery vehicle for bacterial-infected wound areas.

### 3.2. Xyloglucan

Xyloglucans are polysaccharides that are found in the cell walls of terrestrial plants.<sup>118</sup> They undergo reversible sol–gel transitions when degalactosylation is induced by chemical or enzymatic modifications.<sup>119</sup> During degalactosylation, removing galactose residues eliminates the steric hindrance between the branches of xyloglucans and galactose<sup>119,120</sup> (Fig. 7). Consequently, the rod-shaped chains of xyloglucans align into a planar structure, facilitating gelation by forming crosslinked domains upon heating.<sup>97</sup> During this process, the gelation time and gel temperature can be readily controlled based on the extent of galactose removal and the concentration of xyloglucan added, thus rendering it adaptable to diverse fields.<sup>98,121</sup> The optimal removal ratio of galactose residues for forming thermally responsive xyloglucans falls within the range of 35–50%.<sup>97,98</sup> Removal of approximately 45% by weight enables transformation at a biocompatible temperature of 37 °C, facilitating sensitive gelation under physiological conditions.<sup>99,122</sup> This highlights its competitiveness in tissue engineering.<sup>123,124</sup>



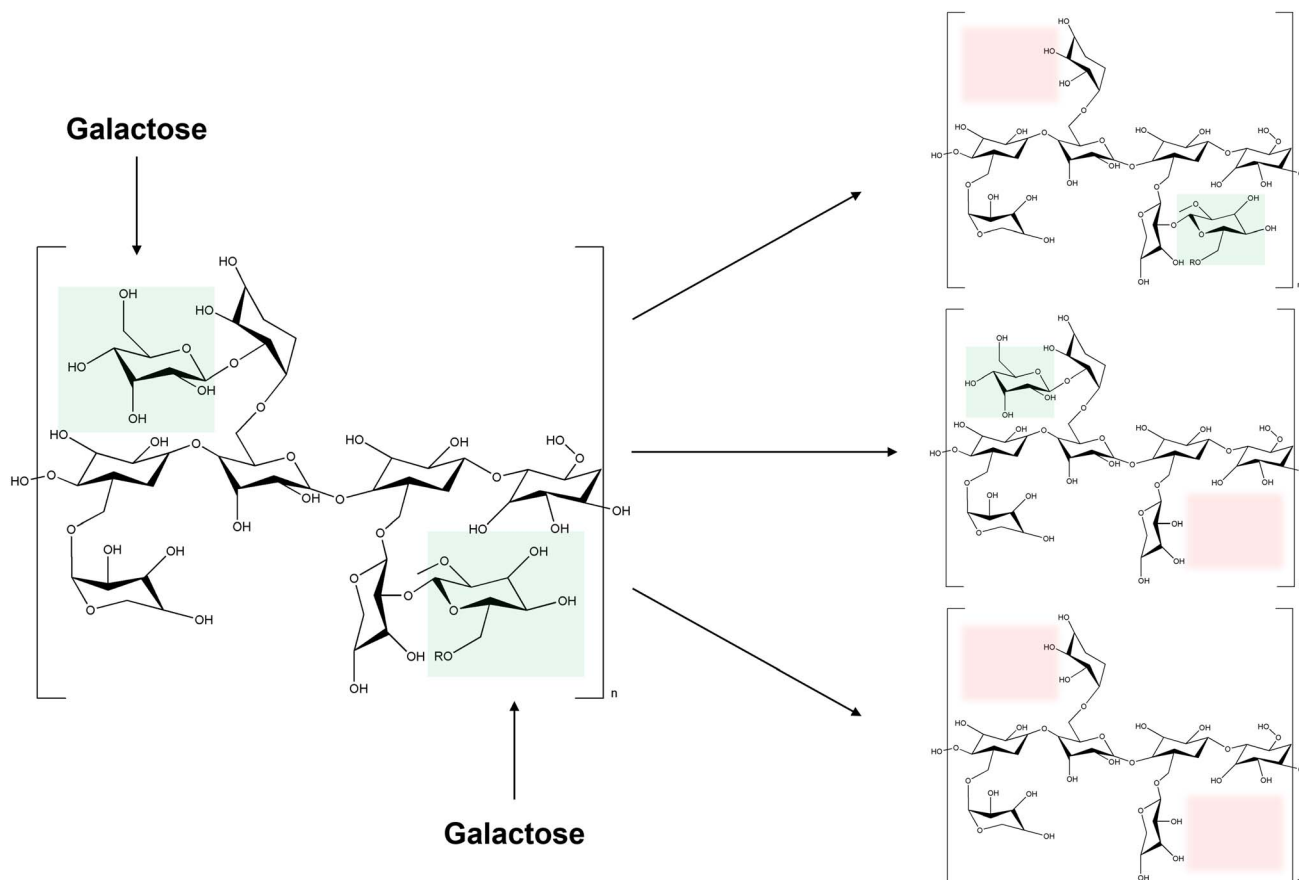


Fig. 7 The mechanism of degalactosylation of xyloglucan (green: galactose, red: possible degalactosylation site).

Xyloglucan, sensitive to biological temperatures, may offer a novel platform for delivering drugs through the nasal cavity to the brain, thereby overcoming application challenges. Xyloglucan has been used to create a nasal thermo-sensitized *in situ* gel for anticonvulsant drug delivery.<sup>125</sup> Gel of all conditions with around 40% degalactosylation gelled at 31–35 °C, enabling *in situ* gelation. Controllable release rates were achieved by adjusting the xyloglucan concentration and drug quantity as observed *in vitro*. The nasal mucosa has excellent perfusion and allows for rapid drug absorption; however, it is crucial to maintain the drug formulation on the mucous membrane for extended periods, as absorption time varies with the administration type.<sup>126</sup> Animal model testing revealed that *in situ* gel formulations persisted longer in the nasal cavity than conventional dosage forms, resisting clearance, and can be controlled to provide a desired drug release in the body. Unlike traditional drug delivery methods such as aqueous suspensions and intravenous boluses, intranasal *in situ* gel formulations significantly enhance brain availability, increasing drug utilization from 31.9% to 90.65%.<sup>125</sup>

Xyloglucan-based *in situ* gels serve not only for drug delivery but also as catalysts for cell growth and tissue formation.<sup>127</sup> Approximately 45% of the degalactosylated xyloglucan is used to create a three-dimensional artificial extracellular matrix, commonly known as a niche.<sup>128–131</sup> Mesenchymal stem cells,

recognized for their multisystem differentiation and regenerative potential, are highly valued in tissue engineering.<sup>132</sup> Culture conditions that provide a stable 3D environment are essential for supporting the growth and functionality of stem cells, which are crucial for advancing regenerative medicine.<sup>127,133,134</sup> This niche offers a nurturing environment for adipose stem cells, promoting their survival and preserving their stemness traits for extended durations of up to 3 weeks.<sup>135,136</sup> Moreover, the gel's injectability has been examined using a needle, demonstrating low viscosity (<0.1 Pa at 25 °C), which enables effortless injection with minimal force, which is particularly vital for applications necessitating direct administration to lesion sites. This injectability is attributed to the pseudoplastic flow behavior of xyloglucan and the reduction in chain entanglements facilitated by incorporating adipose stem cell spheroids.<sup>137</sup> This ensures the viability of the encapsulated cells during the injection process, thereby enhancing the overall efficacy of the *in situ* gel for tissue engineering applications.

Approximately 45% de-galactosylated related glucan prepared an *in situ* gelling hydrogel bound with osteogenic media.<sup>138</sup> When combined with the osteocyte-producing media, the hydrogel exhibited a lower initial modulus than the hydrogel prepared with water, facilitating a more straightforward injection. The sol-gel transition of xyloglucans is triggered by hydrophobic binding interactions and is influenced by ions,



polarities, and hydrophobic solutes in the medium, disrupting chain bonds during gelation when combined with osteogenic media. Here, the viscosity significantly surpasses that of the hydrogel regulated with water in the sol, hindering chain mobility and impeding the formation of interconnected networks.<sup>127</sup> Consequently, despite employing a high polymer concentration, the resulting hydrogel is less rigid than the one mixed with water. This diminishes the network heterogeneity of xyloglucans during extended cultivation. Over time, xyloglucans self-assemble into aggregates and membrane structures, creating a dense porous framework, thereby enhancing rigidity.<sup>127,135</sup>

### 3.3. Methylcellulose

Cellulose is considered one of the most abundant polysaccharides on earth<sup>139,140</sup> and is a backbone polysaccharide consisting of a linear chain of hundreds to thousands of D-glucose units linked by  $\beta(1 \rightarrow 4)$  glycoside bonds.<sup>141,142</sup> Cellulose is derived from various sources, including plants, bacteria, and algae, and can be processed into several variants. One of the modifications, methylcellulose, is the most straightforward cellulose derivative in which a methyl group ( $-\text{CH}_3$ ) replaces a hydroxyl at the C-2, C-3, or C-6 position of the hydro-D-glucose unit (Fig. 8). Methylcellulose has a gelation temperature of 50 to 70 °C,<sup>143</sup> and gelation occurs when heated above that temperature. At low temperatures, hydrogen bonds are formed between hydroxyl groups ( $-\text{OH}$ ) and water molecules in the methylcellulose polymer structure, and a hydration layer is formed surrounding the methyl groups ( $-\text{OCH}_3$ ), maintaining them in a sol state.<sup>100,104</sup> As the temperature rises, the methylcellulose aqueous solution absorbs heat, causing the hydrogen bonds to break and the hydration layer to be lost, resulting in the formation of physically crosslinked gels with intermolecular and intramolecular  $\text{CH}_3-\text{CH}_3$  hydrophobic bonds between the methylcellulose polymers.<sup>100,144</sup> Based on these properties, the gelation temperature can be varied by modifying several factors, including methylcellulose concentration, molecular weight, external stimuli, anions, salt addition, pH changes, and more, enabling gelation at body temperature.<sup>102,103,144-146</sup> These LCST properties of methylcellulose make it useful in various biomedical applications. Methylcellulose maintains a flexible shape or geometry compared to other natural polymers due to the suitable swelling ratio under physiological conditions.<sup>100,147</sup> The gel phase changes with temperature, making it a useful material as a carrier for bioactive components such as cells, drugs, and other bioactive ingredients, making methylcellulose suitable for drug delivery, wound healing, and cell culture.<sup>147</sup>

Methylcellulose is an effective approach for topical drug delivery, which can be used as an *in vivo* gelling delivery system by utilizing its thermo-responsive properties.<sup>148,149</sup> Methylcellulose photo-assisted thermo-responsive methylcellulose hydrogels were developed and used for photo-thermal excision and topical cisplatin delivery.<sup>144</sup> Injection of the drug into the hydrogel reduces injection pain because it is in a soluble phase at room temperature.<sup>144</sup> In addition, photo-assisted conjugation allows gelation in the body temperature range (30 to 60 °C), which prevents drug release to unexpected sites and enables drug delivery to the target site.<sup>100,150</sup> Furthermore, it has suitable shear peeling properties, which reduce the side effects caused by swelling with a swelling rate of less than 40%. When methylcellulose hydrogels containing sodium humate covering target cells were irradiated with light, the cell viability (%) was found to be  $38.63 \pm 1.37$ .<sup>151</sup> This result shows the potential of methylcellulose as a photo-thermal therapy, such as photo-thermal ablation of tumor cells.<sup>144</sup>

Methylcellulose-based *in vivo* gels can be utilized for drug delivery and *in vivo* gels for wound healing applications created within bone. Materials with a short gelation time, which determines the flow of the drug at the injection site, are more advantageous as delivery systems.<sup>152</sup> Therefore, methylcellulose and silk fibroin were used to treat bone disorders. It minimizes cell loss at the injection site, delivers cells to the desired site, and is non-cytotoxic, making it a suitable vehicle for cell therapies. In addition, calcium phosphate incorporated in silk fibroin/methylcellulose-based hydrogels is more likely to promote cell proliferation and differentiation, suggesting that methylcellulose can contribute to the challenge of tissue regeneration.<sup>147</sup> In addition to proteins, bone substitutes have been developed by mixing methylcellulose with calcium phosphate to create hydrogels that gel in place, designed to promote bone substitute phase formation.<sup>153</sup> It can rapidly gelate within 90 seconds at 37 °C and has excellent retention at bone defects, making it a potential thermo-responsive bone substitute.<sup>153</sup> It is superior to conventional hydrogels and scaffolds because it can be implanted through minimally invasive procedures, filling irregularly shaped cavities that often occur after injury or surgery and ensuring continuous integration into host tissue.<sup>154</sup> It has improved mechanical performance and *in vitro* biological characterization has shown the potential to promote cell adhesion, proliferation, and osteogenic differentiation.<sup>100,155</sup>

This ability to adhere and proliferate is also utilized in three-dimensional cell culture models. methylcellulose, hyaluronic acid, and silk fibroin were combined to create a 3D culture

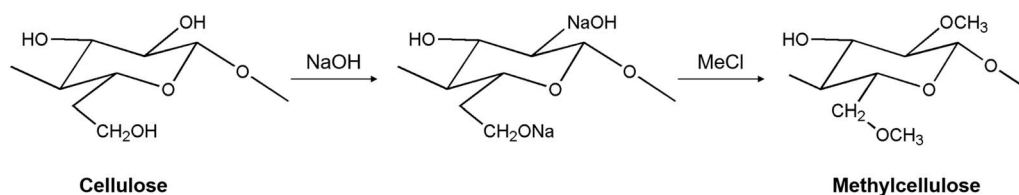


Fig. 8 The mechanism of methylcellulose synthesis.<sup>162</sup>

matrix that mimics the natural extracellular matrix.<sup>156</sup> Homogeneous encapsulation of the cells was easily achieved at 37 °C, and since degradation occurs at room temperature after the formation of multicellular structures, the cells can be recovered from the hydrogel without any desorption agent.<sup>156–160</sup> When evaluated, the hydrogels had an interconnected porous structure, bulky hydrophilicity, high water absorption capacity, *in vitro* stability for up to 6 weeks, and high pore correlation.<sup>160</sup> This allowed us to assess gene and protein expression associated with tumor promotion and identify cell death profiles that could be useful for drug discovery, and the results showed that cell growth and proliferation in the hydrogels was comparable to that observed *in vivo*.<sup>161</sup>

## 4. Conclusions

This review discussed the properties, manufacturing methods, mechanisms, and biomedical applications of thermally reactive polysaccharide-based hydrogels. Hydrogels, crucial in tissue engineering, are predominantly made from synthetic or natural polymers, with natural polymers being favored owing to their high biocompatibility, biodegradability, and bioactivity. Various reactivities are imparted to hydrogels to ensure their controllability within the body. Among these, thermally reactive hydrogels, which undergo sol–gel transitions without being influenced by chemical or environmental factors, have been extensively studied. UCST-reactive polysaccharides, such as agarose, carrageenan, and gellan gum, gel at 30–40 °C, 35–65 °C and 70–90 °C, respectively. Gellan gum has an adjustable gelling temperature of about 37.5 °C, depending on molecular weight and functionalization. These hydrogels have substantial potential for biomedical applications owing to their easily controllable physical properties, straightforward formulation, and characteristic transitions above the critical temperature. Developing UCST hydrogels is beneficial because of the economic feasibility of agarose, ionic reactivity, and advantages of dual crosslinking of carrageenan and gelation at biological temperatures due to the modification of gellan gum. This makes them highly suitable for applications in 3D bioprinting, scaffold production, and drug delivery devices for photo-thermal treatment. In contrast, LCST-reactive polysaccharides, including chitosan and xyloglucan, gel at 32–37 °C and maintain a sol state at lower temperatures. Methylcellulose uniquely gels at temperatures as high as 50–70 °C, but the gelation temperature can be reduced at body temperature by controlling factors such as molecular weight, external stimuli, the addition of anions and salts, and pH changes. The unique advantage of LCST hydrogels lies in their ability to induce *in situ* gelation at physiological temperature (37 °C), which is beneficial for cell culture and stable scaffold production. Consequently, LCST hydrogels are well-suited for producing injectable hydrogels. Leveraging the antimicrobial properties of chitosan, temperature-sensitive reactivity and their mucosal adhesiveness of xyloglucans, proper swelling ability of methylcellulose, these hydrogels exhibit considerable potential for applications in 3D cell sheets, scaffolds for tissue regeneration, and *in situ* gel-based drug delivery systems. Thermally reactive

polysaccharides demonstrate excellent utility in drug delivery, tissue regeneration, and cell culture. They endow hydrogels with unique properties, such as favorable physical characteristics, ease of formulation, and *in vivo* reactivity, making them promising candidates for various biomedical fields.

## Data availability

Data will be made available on request.

## Author contributions

Seo Hyung Moon: conceptualization, investigation, visualization, writing. Sol Ji Park & Ye Won Lee: investigation, visualization, writing. Yun Jung Yang: conceptualization, writing, supervision.

## Conflicts of interest

The authors declare that this study was conducted without commercial or financial relationships that could create conflicts of interest.

## Acknowledgements

The authors acknowledge the financial support from the Inha University Research Grant.

## References

- 1 B. P. Chan and K. W. Leong, *Eur. Spine J.*, 2008, **17**, 467–479.
- 2 M. I. E. Molina, *et al.*, *Front. Bioeng. Biotechnol.*, 2021, **9**, 617141–617170.
- 3 M. C. Socci, *et al.*, *Bioengineering*, 2023, **10**, 218–256.
- 4 S. Bashir, *et al.*, *Polymers*, 2020, **12**, 2702.
- 5 I. M. El-Sherbiny and M. H. Yacoub, *Glob. Cardiol. Sci. Pract.*, 2013, **2013**, 316–343.
- 6 A. Gandini, *et al.*, *Chem. Rev.*, 2016, **116**, 1637–1669.
- 7 T. Zhu, *et al.*, *Adv. Mater. Interfaces*, 2019, **6**, 1900761–1900783.
- 8 L. A. Anholeto, *et al.*, *Microsc. Res. Tech.*, 2018, **81**, 1347–1357.
- 9 Q. Yang, *et al.*, *Carbohydr. Polym.*, 2022, **278**, 118952–118972.
- 10 R. F. Pereira, *et al.*, *Mater. Horiz.*, 2018, **5**, 1100–1111.
- 11 M. I. Rial-Hermida, *et al.*, *ACS Biomater. Sci. Eng.*, 2021, **7**, 4102–4127.
- 12 Z. Li and Z. Lin, *Aggregate*, 2021, **2**, e21.
- 13 W. Wang, *et al.*, *Prog. Polym. Sci.*, 2017, **71**, 1–25.
- 14 Y. Huang, *et al.*, *J. Mater. Sci.*, 2020, **55**, 14690–14701.
- 15 N. Srivastava and A. R. Choudhury, *Ind. Eng. Chem. Res.*, 2023, **62**, 841–866.
- 16 S. Mantha, *et al.*, *Materials*, 2019, **12**, 3323–3356.
- 17 K. Zhang, *et al.*, *Gels*, 2021, **7**, 77–94.
- 18 L. Klouda and A. G. Mikos, *Eur. J. Pharm. Biopharm.*, 2008, **68**, 34–45.



- 19 N. A. Peppas, *et al.*, *Eur. J. Pharm. Biopharm.*, 2000, **50**, 27–46.
- 20 L. Klouda, *Eur. J. Pharm. Biopharm.*, 2015, **97**, 338–349.
- 21 T. Zhang, *et al.*, *Chem. Commun.*, 2024, **60**, 7156–7159.
- 22 Y. Ding, *et al.*, *Polym. Chem.*, 2022, **13**, 2813–2821.
- 23 L. Altomare, *et al.*, *Int. J. Artif. Organs*, 2018, **41**, 337–359.
- 24 N. Srivastava and A. Roy Choudhury, *Carbohydr. Polym.*, 2024, **324**, 121462.
- 25 D. B. Rodrigues, *et al.*, *Biomater. Res.*, 2022, **26**, 1–19.
- 26 L. Schefer, *et al.*, *Biomacromolecules*, 2015, **16**, 985–991.
- 27 B. Neamtu, *et al.*, *Int. J. Mol. Sci.*, 2022, **23**, 9117–9137.
- 28 L. Loukotová, *et al.*, *Carbohydr. Polym.*, 2019, **210**, 26–37.
- 29 Y. Zhang, *et al.*, *Ceram. Int.*, 2014, **40**, 5715–5721.
- 30 C. Soukoulis, *et al.*, *Carbohydr. Polym.*, 2017, **167**, 259–269.
- 31 A. S. Ogrenici, *et al.*, *J. Macromol. Sci., Part B: Phys.*, 2018, **57**, 364–376.
- 32 J. Zhang, *et al.*, *Eur. Polym. J.*, 2023, **199**, 112414–112424.
- 33 Y. Deng, *et al.*, *Small*, 2018, **14**, 1802420–1802430.
- 34 P. Zarrintaj, *et al.*, *Carbohydr. Polym.*, 2018, **187**, 66–84.
- 35 C. Araki, *Bull. Chem. Soc. Jpn.*, 1956, **29**, 543–544.
- 36 X. T. Fu and S. M. Kim, *Mar. Drugs*, 2010, **8**, 200–218.
- 37 M. A. Salati, *et al.*, *Polymers*, 2020, **12**, 1150–1165.
- 38 D. H. Kim, *et al.*, *Appl. Microbiol. Biotechnol.*, 2022, **106**, 8111–8120.
- 39 F. Jiang, *et al.*, *Mar. Drugs*, 2023, **21**, 299–319.
- 40 M. Lahaye and C. Rochas, *Hydrobiologia*, 1991, **221**, 137–148.
- 41 P. D. Benya and J. D. Shaffer, *Cell*, 1982, **30**, 215–224.
- 42 B. Wei, *et al.*, *Biomater. Adv.*, 2024, **160**, 213857–213869.
- 43 M. Hou, *et al.*, *ACS Biomater. Sci. Eng.*, 2018, **4**, 4266–4277.
- 44 G. S. R. Raju, *et al.*, *J. Nanobiotechnology*, 2022, **20**, 1–20.
- 45 H. Veisi, *et al.*, *Int. J. Biol. Macromol.*, 2023, **238**, 124126–124139.
- 46 P. S. Chauhan and A. Saxena, *3 Biotech*, 2016, **6**, 1–18.
- 47 F. Van De Velde, *et al.*, *Carbohydr. Res.*, 2001, **331**, 271–283.
- 48 A. S. Michel, *et al.*, *Int. J. Biol. Macromol.*, 1997, **21**, 195–200.
- 49 N. R. Knudsen, *et al.*, *Mar. Drugs*, 2015, **13**, 3340–3359.
- 50 A. Thakur, *et al.*, *Nanoscale*, 2016, **8**, 12362–12372.
- 51 G. A. De Ruiter and B. Rudolph, *Trends Food Sci. Technol.*, 1997, **8**, 389–395.
- 52 J. Necas and L. Bartosikova, *Vet. Med.*, 2013, **58**, 187–205.
- 53 O. Tari, S. Kara and Ö. Pekcan, *J. Macromol. Sci., Part B: Phys.*, 2009, **48**, 812–822.
- 54 P. Dahal and S. Janaswamy, *Int. Food Res. J.*, 2024, **183**, 114223–114230.
- 55 A. Zhou, *et al.*, *Int. J. Polym. Mater.*, 2023, **72**, 550–560.
- 56 H. Mokhtari, *et al.*, *Polymers*, 2021, **13**, 1744–1765.
- 57 J. Liu, *et al.*, *Carbohydr. Polym.*, 2015, **121**, 27–36.
- 58 A. K. Gaharwar, *et al.*, *ACS Nano*, 2014, **8**, 9833–9842.
- 59 C. F. Candi, *et al.*, *Algal Res.*, 2020, **47**, 101873–101885.
- 60 E. R. Morris, *et al.*, *J. Mol. Biol.*, 1980, **138**, 349–362.
- 61 S. H. Moon, *et al.*, *Mater. Today Bio*, 2024, **25**, 100973–100989.
- 62 J. I. G. Ocampo, *et al.*, *Acta Biomater.*, 2019, **83**, 425–434.
- 63 S. A. Wilson, *et al.*, *ACS Appl. Mater. Interfaces*, 2017, **9**, 43449–43458.
- 64 H. Rastin, *et al.*, *J. Mater. Chem. B*, 2020, **8**, 5862–5876.
- 65 S. Iglauer, *et al.*, *J. Petrol. Sci. Eng.*, 2011, **75**, 304–311.
- 66 K. A. Deo, *et al.*, *Tissue Eng., Part A*, 2020, **26**, 318–338.
- 67 P. Zhuang, *et al.*, *PLoS One*, 2019, **14**, e0216776.
- 68 Y. C. Yeh, *et al.*, *Biofabrication*, 2016, **8**, 045004–045015.
- 69 N. Pettinelli, *et al.*, *Int. J. Pharm.*, 2020, **589**, 119828.
- 70 J. Nourmohammadi, *et al.*, *Mater. Sci. Eng., C*, 2017, **76**, 951–958.
- 71 S. R. Derkach, *et al.*, *LWT–Food Sci. Technol.*, 2015, **63**, 612–619.
- 72 V. T. N. T. Bui, *et al.*, *Food Hydrocolloids*, 2019, **89**, 180–187.
- 73 M. Dionísio and A. Grenha, *J. Pharm. BioAllied Sci.*, 2012, **4**, 175–185.
- 74 R. Yegappan, *et al.*, *Int. J. Biol. Macromol.*, 2019, **122**, 320–328.
- 75 J. S. Varghese, *et al.*, *Colloids Surf., B*, 2014, **113**, 346–351.
- 76 L. W. Doner, *Carbohydr. Polym.*, 1997, **32**, 245–247.
- 77 X. Yang, *et al.*, *Carbohydr. Polym.*, 2024, **345**, 122485.
- 78 R. Chandrasekaran and V. G. Thailambal, *Carbohydr. Polym.*, 1990, **12**, 431–442.
- 79 E. R. Morris, *et al.*, *Food Hydrocolloids*, 2012, **28**, 373–411.
- 80 A. H. Bacelar, *et al.*, *J. Mater. Chem. B*, 2016, **4**, 6164–6174.
- 81 J. J. Kim, *et al.*, *Pharm. Res.*, 2023, **40**, 1491–1505.
- 82 F. S. Palumbo, *et al.*, *Carbohydr. Polym.*, 2020, **229**, 115430.
- 83 C. Villarreal-Otalvaro, *et al.*, *Colloids Surf., B*, 2024, **242**, 114069.
- 84 X. Liu, *et al.*, *Bioact. Mater.*, 2024, **34**, 269–281.
- 85 C. Fiorica, *et al.*, *Int. J. Pharm.*, 2021, **610**, 121231.
- 86 V. Gayathri, N. Pentela and D. Samanta, *Mater. Horiz.*, 2020, 145–181.
- 87 M. I. Gibson and R. K. O'reilly, *Chem. Soc. Rev.*, 2013, **42**, 7204–7213.
- 88 S. R. Majid, *et al.*, *Mol. Cryst. Liq. Cryst.*, 2014, **604**, 84–95.
- 89 A. Baawad, *et al.*, *Tissue Eng., Part B*, 2023, **29**, 123–140.
- 90 T. Osmalek, *et al.*, *Int. J. Pharm.*, 2014, **466**, 328–340.
- 91 H. F. Darge, *et al.*, *Int. J. Biol. Macromol.*, 2019, **133**, 545–563.
- 92 K. Kumar, *et al.*, *ACS Sustain. Chem. Eng.*, 2022, **10**, 9991–10002.
- 93 R. Fan, *et al.*, *Polymers*, 2022, **14**, 2379–2400.
- 94 J. D. dos Santos Carvalho, *et al.*, *Int. J. Biol. Macromol.*, 2022, **209**, 367–375.
- 95 D. Di Lisa, *et al.*, *Biofabrication*, 2023, **16**, 0155011.
- 96 N. H. N. Do, *et al.*, *J. Sol-Gel Sci. Technol.*, 2023, **105**, 451–460.
- 97 M. Shirakawa, K. Yamatoya and K. Nishinari, *Food Hydrocolloids*, 1998, **12**, 25–28.
- 98 D. R. Nisbet, *et al.*, *Biophys. Chem.*, 2006, **121**, 14–20.
- 99 A. K. A. S. B. Graepi, *et al.*, *Carbohydr. Polym.*, 2010, **80**, 555–562.
- 100 L. Bonetti, *et al.*, *Tissue Eng., Part B*, 2021, **27**, 486–513.
- 101 C. H. Chen, *et al.*, *Biomacromolecules*, 2006, **7**, 736–743.
- 102 P. L. Nasatto, *et al.*, *Polymers*, 2015, **7**, 777–803.
- 103 K. Nishinari, *et al.*, *Macromol. Chem. Phys.*, 1997, **198**, 1217–1226.
- 104 N. Sarkar, *J. Appl. Polym. Sci.*, 1979, **24**, 1073–1087.
- 105 L. Yu and J. Ding, *Chem. Soc. Rev.*, 2008, **37**, 1473–1481.
- 106 M. Yamato and T. Okano, *Mater. Today*, 2004, **7**, 42–47.
- 107 X. Liu, *et al.*, *RSC Adv.*, 2017, **7**, 13707–13713.



- 108 S. Islam, *et al.*, *J. Polym. Environ.*, 2016, **25**, 854–866.
- 109 I. Aranaz, *et al.*, *Polymers*, 2021, **13**, 3256–3283.
- 110 T. Irimia, *et al.*, *Mar. Drugs*, 2018, **16**, 373–396.
- 111 J. Amirian, *et al.*, *Carbohydr. Polym.*, 2021, **251**, 117005–117018.
- 112 G. Tan, *et al.*, *Int. J. Biol. Macromol.*, 2017, **103**, 941–947.
- 113 S. P. Balguri, G. R. Adelli and S. Majumdar, *Eur. J. Pharm. Biopharm.*, 2016, **109**, 224–235.
- 114 M. H. Asfour, *et al.*, *Eur. J. Pharm. Sci.*, 2021, **167**, 106041–106051.
- 115 E. I. Rabea, *et al.*, *Biomacromolecules*, 2003, **4**, 1457–1465.
- 116 Z. Aliakbar Ahovan, *et al.*, *Int. J. Biol. Macromol.*, 2020, **164**, 4475–4486.
- 117 R. Chen, *et al.*, *Mar. Life Sci. Technol.*, 2024, **6**, 115–125.
- 118 S. C. Fry, *J. Exp. Bot.*, 1989, **40**, 1–11.
- 119 K. Yamatoya, *et al.*, *J. Funct. Foods*, 2011, **3**, 275–279.
- 120 H. Urakawa, *et al.*, *Trends Glycosci. Glycotechnol.*, 2002, **14**, 355–376.
- 121 J. Esquena-Moret, *Macromol*, 2022, **2**, 562–590.
- 122 S. Todaro, *et al.*, *J. Polym. Sci. Part B: Polym. Phys.*, 2015, **53**, 1727–1735.
- 123 D. U. de Lima and M. S. Buckering, *Carbohydr. Polym.*, 2001, **46**, 157–163.
- 124 E. Zhang, *et al.*, *Acta Biomater.*, 2017, **55**, 420–433.
- 125 A. V. Dalvi, *et al.*, *J. Pharm. Investig.*, 2021, **51**, 199–211.
- 126 H. S. Mahajan, *et al.*, *Drug Deliv.*, 2012, **19**, 270–276.
- 127 F. Toia, *et al.*, *Int. J. Biol. Macromol.*, 2020, **165**, 2886–2899.
- 128 M. Todaro, *et al.*, *Cell Stem Cell*, 2007, **1**, 389–402.
- 129 T. Hoshiba, *et al.*, *Expert Opin. Biol. Ther.*, 2010, **10**, 1717–1728.
- 130 L. E. Fitzpatrick and T. C. McDevitt, *Biomater. Sci.*, 2014, **3**, 12–24.
- 131 K. H. Hong, *et al.*, *Adv. Sci.*, 2019, **6**, 1900597–1900610.
- 132 I. U. Schraufstatter, *et al.*, *Front. Biosci.*, 2011, **16**, 2271–2288.
- 133 A. B. D. Stefano, *et al.*, *Regen. Med.*, 2015, **4**, 100124–100245.
- 134 D. Stefano, *et al.*, *Plast. Surg.*, 2021, **86**, 714–720.
- 135 M. Han, *et al.*, *Carbohydr. Polym.*, 2020, **246**, 116577–116586.
- 136 C. Dispenza, *et al.*, *Cellulose*, 2020, **27**, 3025–3035.
- 137 R. P. Watt, *et al.*, *Int. J. Pharm.*, 2019, **554**, 376–386.
- 138 E. Muscolino, *et al.*, *Mater. Sci. Eng., C*, 2021, **131**, 112545–112560.
- 139 F. Ansari, *et al.*, *Composites, Part A*, 2015, **74**, 60–68.
- 140 R. J. Moon, *et al.*, *Chem. Soc. Rev.*, 2011, **40**, 3941–3994.
- 141 M. Tuomela, *et al.*, *Bioresour. Technol.*, 2000, **72**, 169–183.
- 142 D. M. Updegraff, *Anal. Biochem.*, 1969, **32**, 420–424.
- 143 P. W. Arisz, *et al.*, *Carbohydr. Res.*, 1995, **271**, 1–14.
- 144 F. Ghorbani, *et al.*, *Front. Bioeng. Biotechnol.*, 2022, **10**, 967438.
- 145 T. Sanz, *et al.*, *Food Hydrocolloids*, 2005, **19**, 141–147.
- 146 L. Bonetti, *et al.*, *Mater. Lett.*, 2020, **274**, 128011–128013.
- 147 P. Phewchan, *et al.*, *J. Biomed. Mater. Res., Part B*, 2023, **111**, 1640–1652.
- 148 G. Hou, *et al.*, *Carbohydr. Polym.*, 2022, **276**, 118810–118824.
- 149 A. Luetke, *et al.*, *Cancer Treat. Rev.*, 2014, **40**, 523–532.
- 150 M. C. Tate, *et al.*, *Biomaterials*, 2001, **22**, 1113–1123.
- 151 A. Jhaveri, *et al.*, *J. Controlled Release*, 2014, **190**, 352–370.
- 152 Z. Yin, *et al.*, *RSC Adv.*, 2017, **7**, 24085–24096.
- 153 L. Bonetti, *et al.*, *J. Mater. Chem. B*, 2024, **12**, 4427–4440.
- 154 M. H. Kim, *et al.*, *Int. J. Biol. Macromol.*, 2018, **109**, 57–64.
- 155 G. A. N. Atia, *et al.*, *Pharmaceuticals*, 2023, **16**, 702–738.
- 156 R. Shokri, *et al.*, *Eur. Polym. J.*, 2022, **176**, 111421–111435.
- 157 O. Habanjar, *et al.*, *Int. J. Mol. Sci.*, 2021, **22**, 12200–12234.
- 158 A. Jacob and R. Prekeris, *Front. Cell Dev. Biol.*, 2015, **3**, 4.
- 159 O. Tolde, *et al.*, *Eur. J. Cell Biol.*, 2010, **89**, 674–680.
- 160 T. Azimi, *et al.*, *Sci. Rep.*, 2020, **10**, 12020–12030.
- 161 Z. Huang, *et al.*, *OncoTargets Ther.*, 2020, **13**, 5395–5405.
- 162 E. Saiki, *et al.*, *ACS Omega*, 2022, **7**, 28849–28859.
- 163 S. S. Jain, *et al.*, *J. Appl. Pharm. Sci.*, 2013, **3**, 139–144.

